ORIGINAL ARTICLE

Hepatic Shunting of Eggs and Pulmonary Vascular Remodeling in *Bmpr2*$^{+/-}$ Mice with Schistosomiasis

Alexi Crosby[1]*, Elaine Soon[1]*, Frances M. Jones[2], Mark R. Southwood[3], Leila Haghighat[1], Mark R. Toshner[1], Tim Raine[1], Ian Horan[1], Peiran Yang[1], Stephen Moore[1], Elisabet Ferrer[1], Penny Wright[4], Mark L. Ormiston[1], R. James White[5], Deborah A. Haight[5], David W. Dunne[2], and Nicholas W. Morrell[1]

[1]Department of Medicine, University of Cambridge School of Clinical Medicine, Addenbrooke's Hospital, Cambridge, United Kingdom; [2]Department of Pathology, University of Cambridge, Cambridge, United Kingdom; [3]Department of Pathology, Papworth Hospital, Cambridge, United Kingdom; [4]Addenbrooke's Hospital, Cambridge, United Kingdom; and [5]University of Rochester, Rochester, New York

ORCID ID: 0000-0001-5063-961X (A.C.).

Abstract

Rationale: Schistosomiasis is a major cause of pulmonary arterial hypertension (PAH). Mutations in the bone morphogenetic protein type-II receptor (BMPR-II) are the commonest genetic cause of PAH.

Objectives: To determine whether *Bmpr2*$^{+/-}$ mice are more susceptible to schistosomiasis-induced pulmonary vascular remodeling.

Methods: Wild-type (WT) and *Bmpr2*$^{+/-}$ mice were infected percutaneously with *Schistosoma mansoni*. At 17 weeks postinfection, right ventricular systolic pressure and liver and lung egg counts were measured. Serum, lung and liver cytokine, pulmonary vascular remodeling, and liver histology were assessed.

Measurements and Main Results: By 17 weeks postinfection, there was a significant increase in pulmonary vascular remodeling in infected mice. This was greater in *Bmpr2*$^{+/-}$ mice and was associated with an increase in egg deposition and cytokine expression, which induced pulmonary arterial smooth muscle cell proliferation, in the lungs of these mice. Interestingly, *Bmpr2*$^{+/-}$ mice demonstrated dilatation of the hepatic central vein at baseline and postinfection, compared with WT. *Bmpr2*$^{+/-}$ mice also showed significant dilatation of the liver sinusoids and an increase in inflammatory cells surrounding the central hepatic vein, compared with WT. This is consistent with an increase in the transhepatic passage of eggs.

Conclusions: This study has shown that levels of BMPR-II expression modify the pulmonary vascular response to chronic schistosomiasis. The likely mechanism involves the increased passage of eggs to the lungs, caused by altered diameter of the hepatic veins and sinusoids in *Bmpr2*$^{+/-}$ mice. Genetically determined differences in the remodeling of hepatic vessels may represent a new risk factor for PAH associated with schistosomiasis.

Keywords: pulmonary hypertension; schistosomiasis; bone-morphogenetic protein type II receptor; pulmonary vascular remodeling

Schistosomiasis is the world's third leading endemic parasitic disease and is reputedly the world's most common cause of pulmonary arterial hypertension (PAH) (1). After infection, *Schistosoma mansoni* worms mate in the liver and lay eggs in the mesenteric venules of the intestine. Most eggs are excreted in the stool; however, some are retained in the tissues and migrate to hepatic sinusoids. Chronic *S. mansoni* infection can result in periportal fibrosis and portal hypertension; portocaval collaterals are thought to enlarge, allowing eggs to embolize to the lung, where they migrate through the vessel wall into the

(Received in original form December 18, 2014; accepted in final form August 9, 2015)

*These authors contributed equally to this manuscript.

Supported by the British Heart Foundation and the Wellcome Trust (096822/Z/11/Z; P.Y.).

Author Contributions: A.C., F.M.J., E.S., M.R.S., M.R.T., L.H., T.R., I.H., S.M., E.F., P.W., P.Y., D.A.H., M.L.O., and R.J.W. were involved with acquisition, analysis, or interpretation of the data. A.C., F.M.J., D.W.D., and N.W.M. contributed to the design and the conception of the study and interpretation of the data. All authors were involved with drafting/revising and approving the manuscript.

Correspondence and requests for reprints should be addressed to Nicholas W. Morrell, M.D., Division of Respiratory Medicine, Department of Medicine, University of Cambridge School of Clinical Medicine, Box 157, Addenbrooke's Hospital, Hills Road, Cambridge CB2 0QQ, UK. E-mail: nwm23@cam.ac.uk

This article has an online supplement, which is accessible from this issue's table of contents at www.atsjournals.org

Am J Respir Crit Care Med Vol 192, Iss 11, pp 1355–1365, Dec 1, 2015

Originally Published in Press as DOI: 10.1164/rccm.201412-2262OC on August 26, 2015
Internet address: www.atsjournals.org

At a Glance Commentary

Scientific Knowledge on the Subject: Schistosomiasis is considered the commonest worldwide cause of pulmonary arterial hypertension (PAH). Mutations in the bone morphogenetic protein type-II receptor (BMPR-II) are the commonest genetic cause of PAH. However, little is known as to whether mutations in BMPR-II can increase susceptibility to schistosomiasis-induced pulmonary vascular remodeling and PAH.

What This Study Adds to the Field: We used our established model of chronic schistosomiasis in wild-type and *Bmpr2*$^{+/-}$ mice and showed that animals deficient in BMPR-II demonstrate a greater number of eggs and higher cytokine expression in the lungs, associated with a greater degree of pulmonary vascular remodeling. In addition, we show that the increased lung egg deposition is caused by a greater diameter of the hepatic veins and sinusoids in *Bmpr2*$^{+/-}$ mice. Thus, genetically determined differences in the hepatic vasculature may represent a new risk factor for PAH associated with schistosomiasis.

parenchyma (2, 3), resulting in the formation of granulomata with subsequent fibrosis (4).

Until recently, it was unclear whether pulmonary vascular remodeling and PAH in schistosomiasis was caused by the presence of eggs in the lung, the underlying liver disease, or systemic inflammation. However, recent studies by our group and others (5–8) in mouse models have shown that pulmonary vascular remodeling and PAH are related to the density of egg deposition within the lung and the subsequent local inflammatory reaction, which induces pulmonary arterial smooth muscle cell (PASMC) proliferation. In addition, we have shown (6) that the local inflammatory cytokines, particularly IL-13, induce migration of PASMC, thus contributing to pulmonary vascular remodeling. We have observed a negative correlation between egg distance and degree of vascular remodeling (5). Transforming growth factor (TGF)-β signaling seems to be particularly important in driving the remodeling.

Although the mechanisms underlying the pathobiology of PAH are diverse (9–11) a central mechanism involves mutations in bone morphogenetic protein type-II receptor (BMPR-II), a receptor for the TGF-β superfamily (9, 12–15). Mutations in BMPR-II are known to cause 80% of cases of familial and up to 25% of sporadic cases of PAH. Dysfunction of BMPR-II signaling has been shown by our group (9, 16, 17) and others (14, 15) to contribute to nongenetic forms of pulmonary hypertension in humans (16, 18, 19) and experimental animal models.

The aim of the present study was to determine if *Bmpr2*$^{+/-}$ mice developed more profound pulmonary vascular remodeling compared with wild-type (WT) mice, and if so, what mechanisms underlie this process. We found that *Bmpr2*$^{+/-}$ mice exhibited more pronounced vascular remodeling than WT mice; this was associated with a significant increase in egg burden in the lungs of these animals. Because hepatic vein shunting of eggs is thought to be the mechanism of egg deposition in the lung during *Schistosoma* spp. infection we looked for and found evidence not only of dilatation of the hepatic veins in *Bmpr2*$^{+/-}$ mice but also dilation of the hepatic sinusoids and an increase in neutrophils surrounding the hepatic vessels, thus providing an explanation for the mechanism of egg transit to the lungs. Thus, genetically determined differences in the portal vasculature may contribute to the pathobiology of PAH associated with schistosomiasis.

Methods

Experimental Mouse Model of *S. mansoni* Infection

A Puerto Rican strain of *S. mansoni* was used in all experiments (20). Thirteen

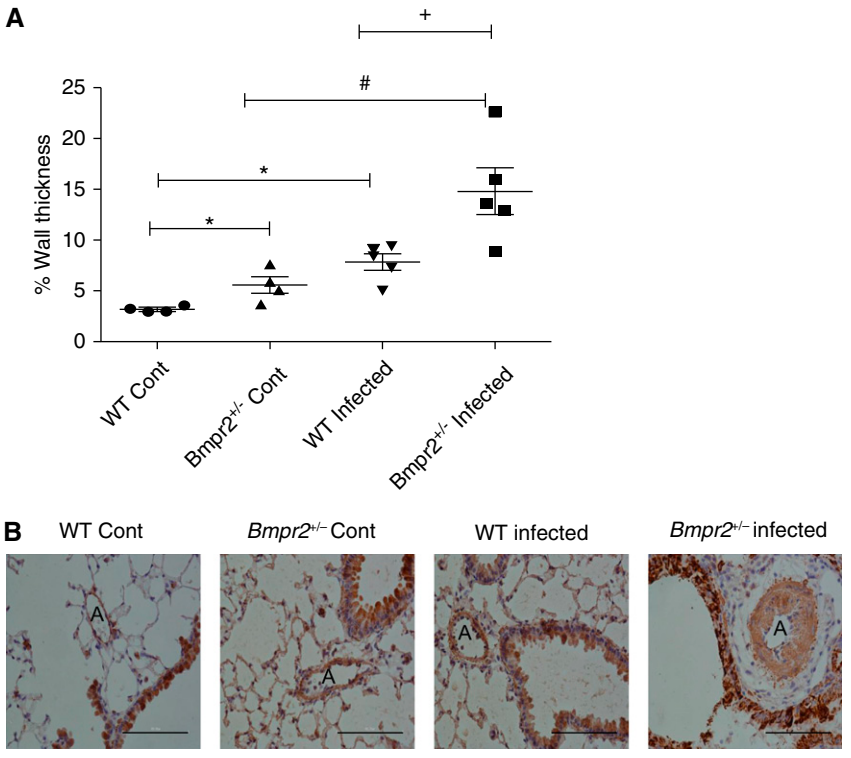

Figure 1. (*A*) Scatter plot showing percentage wall thickness of pulmonary arterioles at the level of the terminal bronchiole in wild-type (WT) control (n = 4), *Bmpr2*$^{+/-}$ control (n = 4), WT infected (n = 5), and *Bmpr2*$^{+/-}$ infected lungs (n = 5). Data are presented as mean ± SEM. $^{*}P < 0.05$ compared with WT control, $^{\#}P < 0.05$ compared with *Bmpr2*$^{+/-}$ control, $^{+}P < 0.05$ compared with WT infected. (*B*) Representative photomicrographs ×400 magnification of lung sections immunostained with α-smooth muscle actin from WT control, *Bmpr2*$^{+/-}$ control, WT infected, and *Bmpr2*$^{+/-}$ infected mice. *Scale bars* = 100 μm. A = arteries; Bmpr2 = bone morphogenetic protein type 2 receptor; Cont = control.

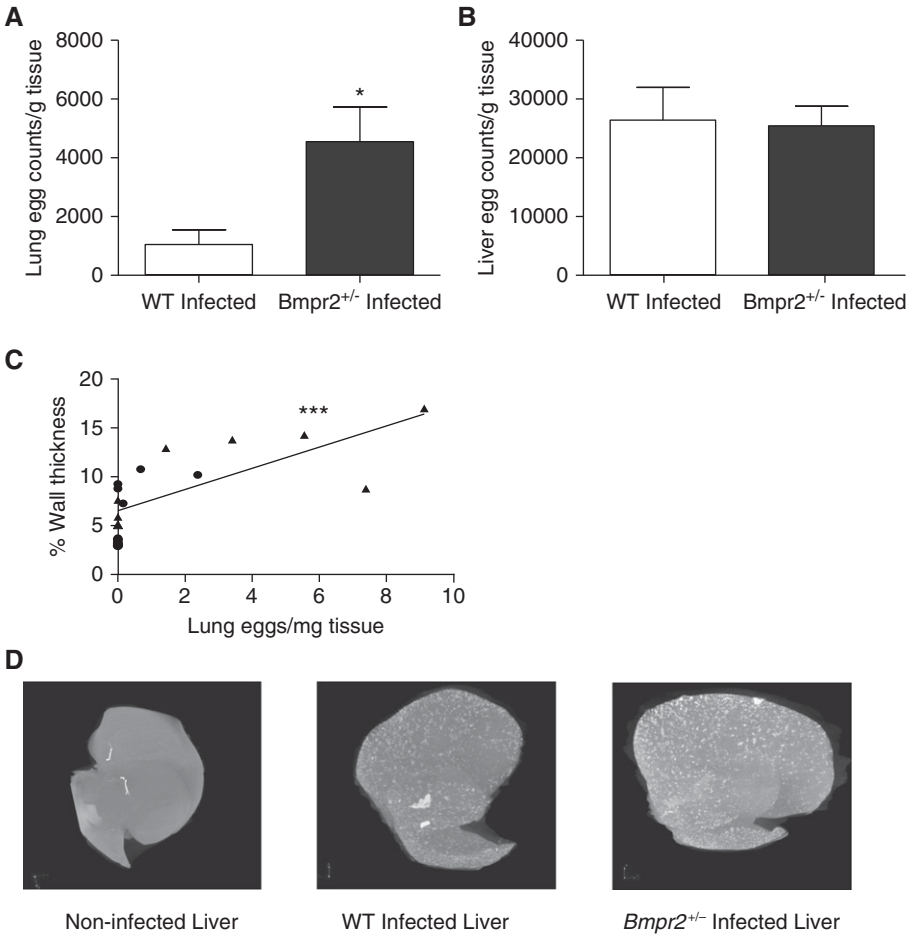

Figure 2. (*A*) Lung egg count per gram of tissue in wild-type (WT) infected (n = 9) and *Bmpr2*$^{+/-}$ infected (n = 7) mice. Data are presented as mean ± SEM. *$P < 0.05$. (*B*) Liver egg counts per gram of tissue (n = 10), WT infected (n = 10), and *Bmpr2*$^{+/-}$ infected (n = 8) mice. Data are presented as mean ± SEM. (*C*) Correlation between percentage wall thickness and lung eggs in WT (*circles*) and *Bmpr2*$^{+/-}$ (*triangles*) mice (slope = 1.085; 95% confidence interval, 0.5228–1.647; ***$P < 0.001$; $r = 0.65$ Spearman correlation coefficient). (*D*) Micro–computed tomography of a noninfected mouse liver and a WT and *Bmpr2*$^{+/-}$ infected liver. Bmpr2 = bone morphogenetic protein type 2 receptor.

female BMPR-II heterozygous (*Bmpr2*$^{+/-}$) and 16 female WT (littermate control animals) C57/BL6 adult mice were infected transcutaneously with 30 cercariae, as previously described (6). At 17 weeks postinfection animals underwent right heart catheterization and were then killed. Mice were exsanguinated and plasma was retained for cytokine analysis. Noninfected WT and *Bmpr2*$^{+/-}$ animals were also studied. All protocols and surgical procedures were approved by the local animal care committee.

Measurement of Right Ventricular Systolic Pressure

At 17 weeks postinfection mice were anesthetized (hypnorm/hypnovel) for hemodynamic assessment. Body weight was recorded and right-heart catheterization was performed to measure right ventricular systolic pressure, as previously described (21).

Right Ventricular Hypertrophy

The degree of right ventricular hypertrophy was determined from the RV/(LV + S) ratio, as previously described (21).

Tissue Preparation

The left lung was fixed *in situ* in the distended state by infusion of 0.8% agarose into the trachea, and then placed in 10% paraformaldehyde before paraffin-embedding. The right caudal lobe was taken for egg counts. The remaining lung lobes were frozen in liquid nitrogen. The liver was removed and weighed. The right, caudate, and left lateral lobes of the liver were retained for egg counts. Liver was also placed in 10% paraformaldehyde for histology and immunocytochemistry.

Tissue Egg Counts

To quantify the number of eggs in the lung and liver, tissues were digested in 4% KOH, and eggs were counted as described previously (22).

Pulmonary Vascular Morphometry

Lung tissues were stained with anti–smooth muscle α-actin (DakoCytomation, Ely, UK) (*see* online supplement methods).

Micro–Computed Tomography

Micro–computed tomography on the livers of control and infected mice inflated lungs was performed using a Skyscan 1174 (Bruker Instruments, Kontich, Belgium) (*see* online supplement methods).

Liver Morphometry

Liver tissue was placed in formalin and processed as previously described (*see* online supplement methods) (23).

Collagen Assay

A collagen assay (as previously described [24]) was performed to measure the degree of fibrosis in the liver and lungs of control and infected mice.

Cytokine Measurements

Serum cytokines levels were measured using a multiplexed mouse cytokine assay from R and D Systems (Abingdon, UK) according to the manufacturer's protocol. Lung and liver cytokine mRNA expression was determined after TRIzol extraction using real-time polymerase chain reaction (*see* online supplement methods). Protein levels of lung cytokines were measured using the MSD Multispot assay (Meso Scale Diagnostics, Rockville, MD).

Macrophage Phagocytosis Assay

A macrophage phagocytosis assay was performed (*see* online supplement methods).

Statistical Analysis

GraphPad Prism 5 (GraphPad Software, Inc., La Jolla, CA) was used for all statistical analysis. Where appropriate, data were tested for normality using the Kolmogorov-Smirnov method. Where the data were not

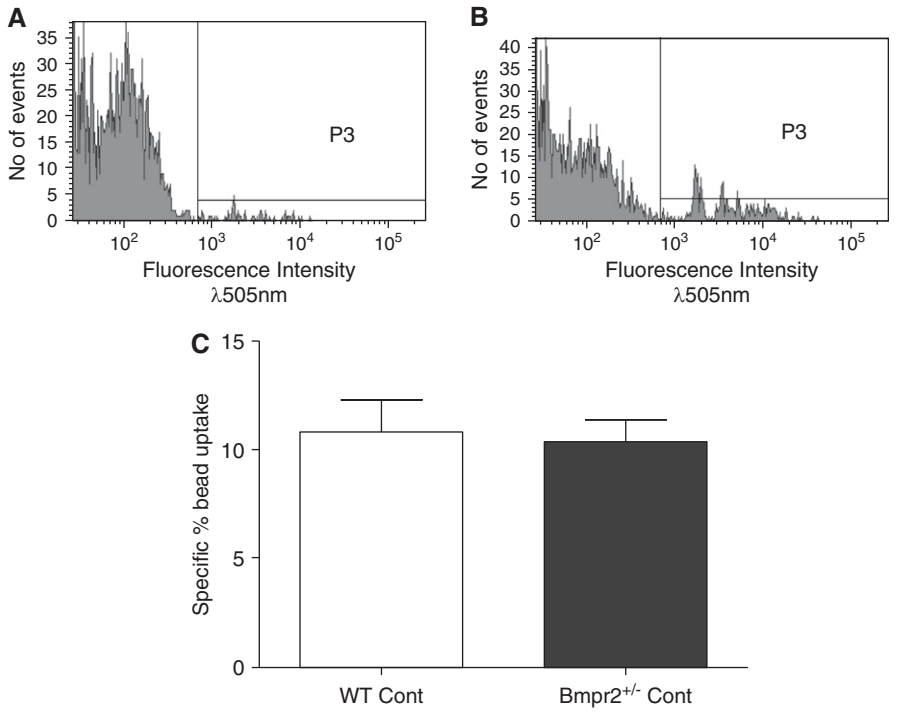

Figure 3. (*A*, *B*) Plots showing fluorescence of macrophages cultured with fluorescently tagged beads for 2 hours at 4°C (P3) (control) (*A*) and macrophages cultured with fluorescently tagged beads for 2 hours at 37°C (P3) (experimental) (*B*). (*C*) Bar chart showing percentage of specific bead uptake in macrophages from wild-type (WT) and *Bmpr2*$^{+/-}$ control mice, calculated as fluorescence at 37°C (P3) − fluorescence at 4°C (P3). Graph shows mean ± SEM of four individual experiments. Bmpr2 = bone morphogenetic protein type 2 receptor; Cont = control; P3 = fluorescence intensity above background.

normally distributed nonparametric analysis was applied. Data are presented as mean ± SEM. Data were compared using the Mann-Whitney (Figures 1, 2A, 3C, 4A, 6A–6D, 6G, 7, 8A, 8C, 8D, and 9) or Student *t* test (Figures 2B, 4B, 6F, and 7B) as appropriate. Correlations were determined using Spearman rank correlation, linear regression (Figures 2C and 6E). The level of significance was *P* less than 0.05.

Results

Bmpr2$^{+/-}$ Mice Develop More Marked Pulmonary Vascular Remodeling Than WT Mice

To determine if mutant schistosomiasis-infected mice develop more profound remodeling we measured percentage wall thickness of pulmonary vessels associated with terminal bronchioles. The data show that WT and *Bmpr2*$^{+/-}$ infected mice develop a significant elevation in percentage medial wall thickness when compared with their noninfected WT and *Bmpr2*$^{+/-}$ ($P < 0.05$, respectively) (Figure 1A). The *Bmpr2*$^{+/-}$ infected mice had a significantly greater percentage wall thickness ($P < 0.05$) compared with WT infected mice (Figure 1A). Interestingly, even at baseline, *Bmpr2*$^{+/-}$ noninfected mice exhibited a significantly greater percentage wall thickness, compared with WT noninfected mice. Despite the increase in pulmonary vascular remodeling seen, we did not see an increase in right ventricular systolic pressure, right ventricular hypertrophy, or liver weight in *Bmpr2*$^{+/-}$ mice compared with WT mice (*see* Figure E1 in the online supplement). This is consistent with our previous findings where at least 25 weeks of infection is needed for animals to develop overt PAH (5). Figure 1B shows representative photomicrographs of lung sections taken for analysis.

Bmpr2$^{+/-}$ Mice Exhibit Increased Egg Deposition in the Lungs, Which Correlates with Vascular Wall Thickness

Our previous studies have shown that it is the presence of eggs in the lungs that is responsible for the pulmonary vascular remodeling seen in this model of PAH (5, 6). Moreover, we have shown that the degree of vascular remodeling correlates negatively with the distance of the vessel from the egg (5). Interestingly, the *Bmpr2*$^{+/-}$ mice exhibited increased numbers of eggs in the lung compared with WT mice ($P < 0.05$) (Figure 2A). Consistent with our previous reports, we have confirmed the positive correlation between lung egg burden and pulmonary vessel thickness (in both WT and *Bmpr2*$^{+/-}$ mice) ($P < 0.001$; linear regression model; regression coefficient, 1.085; 95% confidence interval, 0.5228–1.647; Spearman rank correlation coefficient) (Figure 2C).

In contrast to the differences between genotypes in the number of eggs in the lungs, there was no difference in the number of eggs in the liver tissue between the *Bmpr2*$^{+/-}$ and WT mice (Figure 2B). As previously reported (5, 6), the overall number of eggs in the liver was approximately 10-fold higher than the number of eggs in the lung. Micro–computed tomography revealed the similar distribution of granulomata surrounding eggs in the livers of WT and *Bmpr2*$^{+/-}$ animals (Figure 2D). The degree of fibrosis in the lung and liver tissue was determined using a colorimetric assay (*see* Figure E2). There was a significant increase in fibrosis in the livers and lungs of infected mice compared with noninfected mice but no difference between the genotypes.

Macrophages from *Bmpr2*$^{+/-}$ Mice Do Not Demonstrate Defects in Phagocytosis

To determine if the increased egg deposition in the lungs of the *Bmpr2*$^{+/-}$ mice could be related to a defect in macrophage phagocytosis, we cultured macrophages from WT and *Bmpr2*$^{+/-}$ mice with fluorescently tagged beads and measured their ability to phagocytose the beads (Figures 3A and 3B). There were no differences in the ability of bone-marrow-derived macrophages from *Bmpr2*$^{+/-}$ or WT mice to phagocytose beads (Figure 3C).

Bmpr2$^{+/-}$ Mice Exhibit Dilatation of Hepatic Veins and Sinusoids

To identify the mechanism for increased lung deposition of eggs in *Bmpr2*$^{+/-}$ mice we hypothesized that BMPR-II deficiency may alter hepatic vascular structure because (*1*) BMPR-II plays an important role in vascular integrity (25, 26), (*2*) BMPR-II

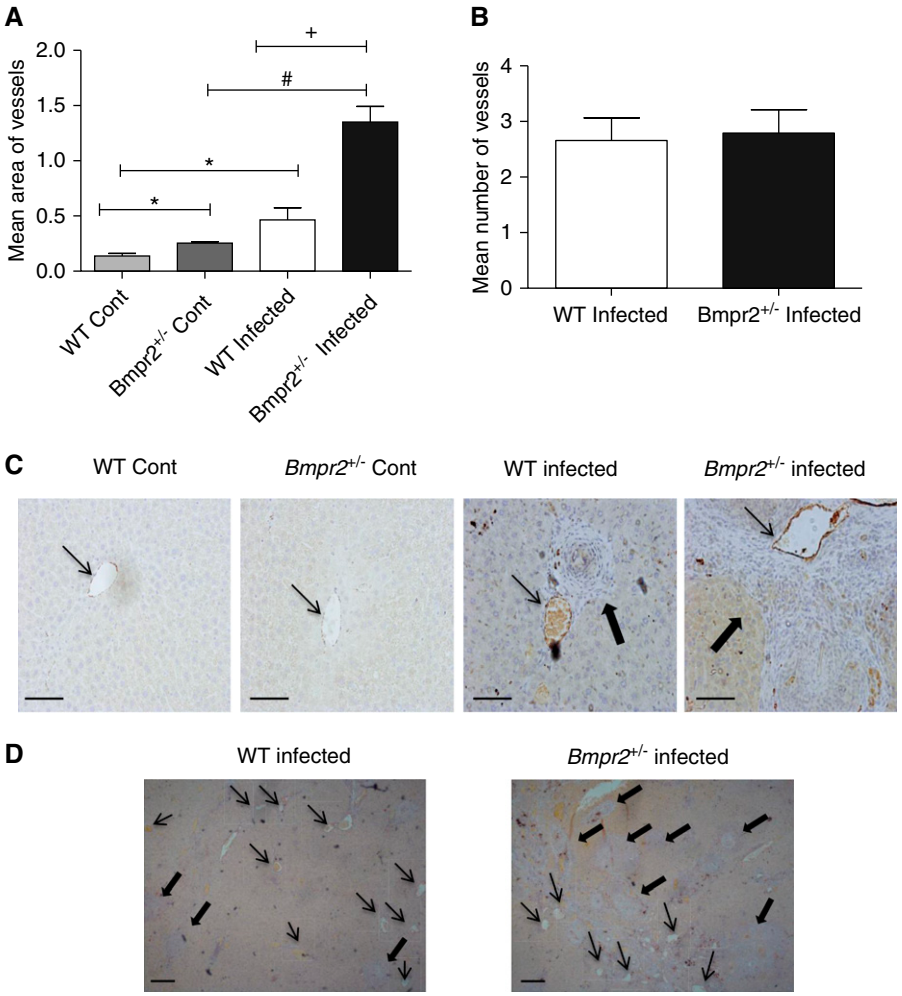

Figure 4. (*A*) Quantification of mean vessel area (±SEM) of central hepatic veins in liver sections of wild-type (WT) (n = 4) and *Bmpr2*$^{+/-}$ (n = 4) control and infected mice. *$P < 0.05$ compared with WT control, $^{\#}P < 0.05$ compared with *Bmpr2*$^{+/-}$ control, $^{+}P < 0.05$ compared with WT infected. (*B*) Quantification of the mean ± SEM number of vessels in the liver of WT (n = 5) and *Bmpr2*$^{+/-}$ (n = 6) infected mice. (*C*) Photomicrographs of von Willibrand factor–stained liver sections of WT and *Bmpr2*$^{+/-}$ control and infected mice at ×200 magnification. *Scale bars* = 100 μm. (*D*) Photomicrographs of von Willibrand factor–stained liver sections of WT and *Bmpr2*$^{+/-}$ infected mice at ×40 magnification. *Scale bars* = 100 μm. *Thin arrows*, hepatic central veins; *thick arrows*, granulomas. Bmpr2 = bone morphogenetic protein type 2 receptor; Cont = control.

mutation has been associated with arteriovenous malformations (27), and (3) portocaval collateral vessels are thought to be the conduit for the passage of schistosoma eggs to the lung (2, 3). In support of our hypothesis, we observed a small but significant increase in the diameter of the central hepatic veins in noninfected *Bmpr2*$^{+/-}$ mice (Figures 4A and 4C) compared with WT mice. The diameter of the hepatic veins was increased in WT and *Bmpr2*$^{+/-}$ mice chronically infected with *S. mansoni* (Figures 4A, 4C, and 4D). However, dilatation of hepatic veins was more marked in infected *Bmpr2*$^{+/-}$ mice compared with infected WTs (Figures 4A, 4C, and 4D). There was a significant increase in the number of neutrophils ($P < 0.05$) surrounding the hepatic veins in the infected mice compared with noninfected mice (*see* Figure E3A). There was a trend ($P = 0.05$) for an increase in neutrophils surrounding the hepatic central vein in infected *Bmpr2*$^{+/-}$ mice, compared with infected WT mice (*see* Figure E3B). In addition, there was a significant dilatation of the hepatic sinusoids in *Bmpr2*$^{+/-}$ infected mice compared with noninfected *Bmpr2*$^{+/-}$ mice, and compared with WT infected mice (Figure 5). There was no increase in vessel number in infected *Bmpr2*$^{+/-}$ mice, compared with WT mice (Figure 4B).

Bmpr2$^{+/-}$ Mice Demonstrate Increased Lung IL-13 Expression

We have previously shown that chronic schistosomiasis and lung egg deposition causes an increase in the expression of cytokines in the mouse lung, especially IL-13, keratinocyte chemoattractant (Kc), and IL-4, and that lung cytokines correlate with egg burden and degree of pulmonary vascular remodeling (5, 6). In the present study we compared lung IL-6, IL-8, and IL-13 mRNA expression in *Bmpr2*$^{+/-}$ and WT mice after 17 weeks of infection to determine whether *Bmpr2*$^{+/-}$ mice demonstrate increased local lung cytokine expression.

In keeping with the increased egg burden seen in the lungs of the *Bmpr2*$^{+/-}$ mice, we observed an increase in IL-13 mRNA expression ($P < 0.05$) (Figure 6A) and a trend toward an increase in IL-6 expression in the lungs of these mice, compared with WT mice. There was a high degree of variability between the animals in lung expression of Kc and IL-4 (Figures 6B and 6C, respectively). We found a significant increase in both lung expression of IL-13 and IL-6 ($P < 0.05$) in the infected *Bmpr2*$^{+/-}$ mice compared with *Bmpr2*$^{+/-}$ control. We found a significant correlation between lung IL-13 mRNA

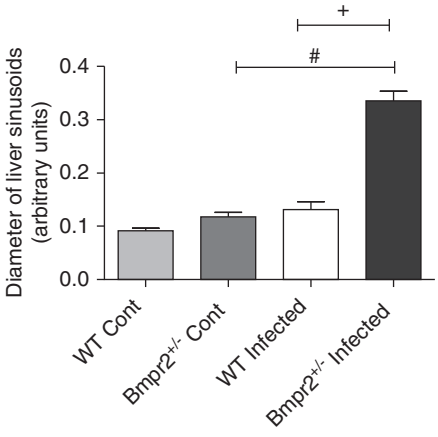

Figure 5. Bar graph showing hepatic sinusoid diameter in wild-type (WT) and *Bmpr2*$^{+/-}$ control (n = 4) and WT and *Bmpr2*$^{+/-}$ infected mice (n = 5). Data are presented as mean ± SEM. $^{\#}P < 0.05$ compared with *Bmpr2*$^{+/-}$ control, $^{+}P < 0.05$ compared with WT infected. Bmpr2 = bone morphogenetic protein type 2 receptor; Cont = control.

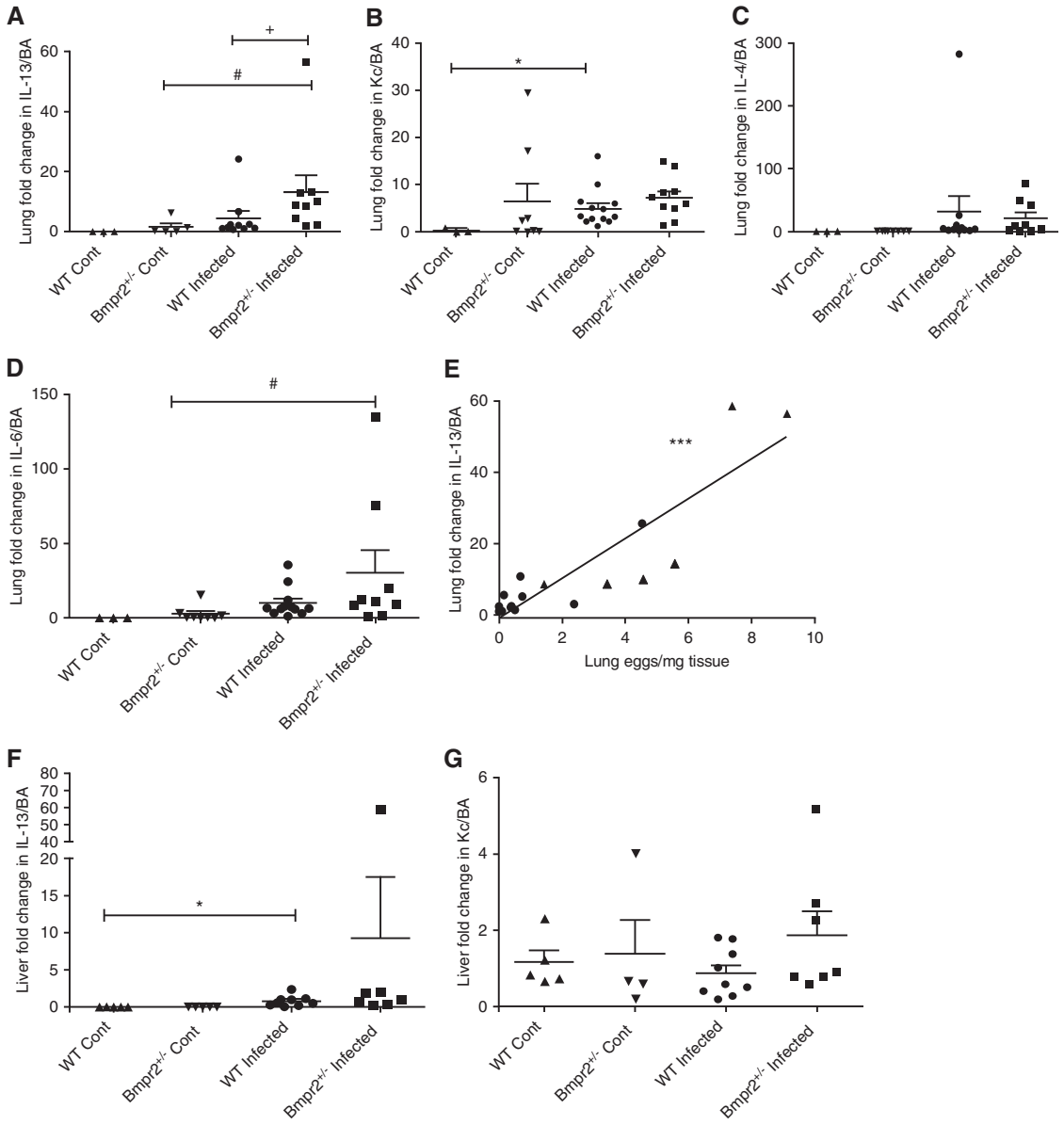

Figure 6. (*A–D*) Plots showing lung cytokine expression in wild-type (WT) and *Bmpr2*$^{+/-}$ control and infected mice. (*A*) IL-13 (WT Cont n = 3, *Bmpr2*$^{+/-}$ Cont n = 5, WT infected n = 10, *Bmpr2*$^{+/-}$ infected n = 9); (*B*) keratinocyte chemoattractant (Kc) (WT Cont n = 3, *Bmpr2*$^{+/-}$ Cont n = 8, WT infected n = 13, *Bmpr2*$^{+/-}$ infected n = 10); (*C*) IL-4 (WT Cont n = 3, *Bmpr2*$^{+/-}$ Cont n = 8, WT infected n = 11, *Bmpr2*$^{+/-}$ infected n = 9); (*D*) IL-6 (WT Cont n = 3, *Bmpr2*$^{+/-}$ Cont n = 8, WT infected n = 12, *Bmpr2*$^{+/-}$ infected n = 9). Data are presented as mean ± SEM. $^{\#}P < 0.05$ compared with *Bmpr2*$^{+/-}$ control, $^{+}P < 0.05$ compared with WT infected, and $^{*}P < 0.05$ compared with WT control. (*E*) Correlation between lung IL-13 expression and lung egg deposition (n = 17) (Spearman rank correlation coefficient in WT [*circles*] and *Bmpr2*$^{+/-}$ [*triangles*] infected mice, $^{***}P < 0.001$). (*F*, *G*) Liver cytokine expression in WT and *Bmpr2*$^{+/-}$ control and infected mice. (*F*) IL-13 (WT Cont n = 6, *Bmpr2*$^{+/-}$ Cont n = 6, WT infected n = 9, *Bmpr2*$^{+/-}$ infected n = 7); (*G*) Kc (WT Cont n = 5, *Bmpr2*$^{+/-}$ Cont n = 4, WT infected n = 9, *Bmpr2*$^{+/-}$ infected (n = 7). Data are presented as mean ± SEM. $^{*}P < 0.05$ compared with WT control. Bmpr2 = bone morphogenetic protein type 2 receptor; Cont = control.

expression and the number of eggs in the lung ($P < 0.001$) (Figure 6E). There were no significant differences in the expression levels of these cytokines in the livers of infected animals (Figures 6F and 6G), in keeping with the similar liver egg deposition. In addition, we saw a significant increase in IL-12p70, IL-2, and IL-4 protein expression in the lungs of infected mice compared with noninfected mice ($P < 0.05$) (Figures 7A–7C). We also observed a significant reduction in IL-12p70 levels in infected *Bmpr2*$^{+/-}$ mice compared with WT infected mice. Interestingly, IL-12P70 plays an important immunomodulatory role and has been shown to down-regulate granuloma formation (28). There was no significant difference in the levels of circulating serum cytokines between WT and *Bmpr2*$^{+/-}$ infected mice (Figure 8). However, we did observe a significant increase in serum

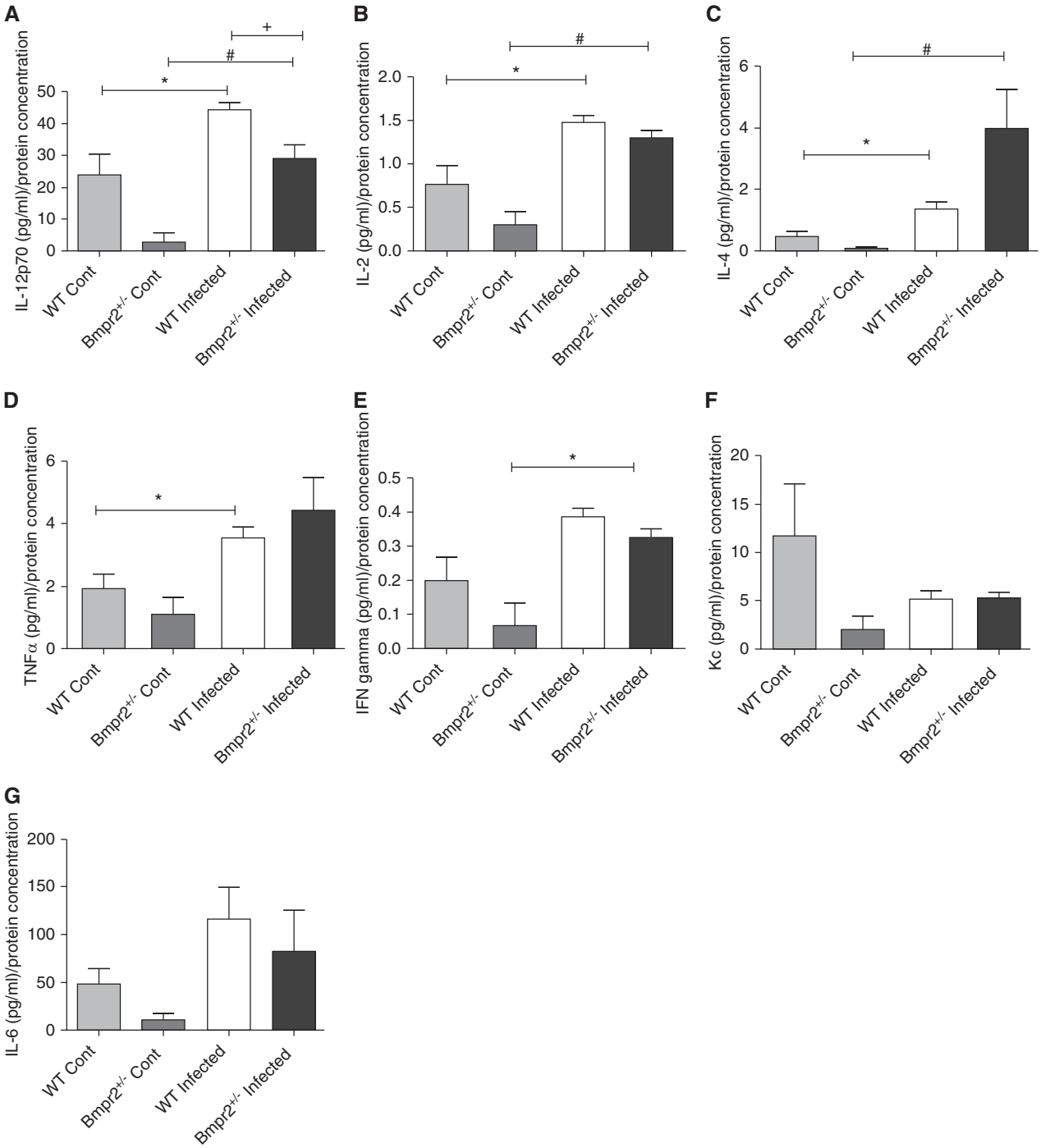

Figure 7. Bar graphs showing lung cytokine profiles in wild-type (WT) and *Bmpr2*$^{+/-}$ control and infected mice. (*A*) IL-12p70; (*B*) IL-2; (*C*) IL-4; (*D*) tumor necrosis factor (TNF)-α; (*E*) IFN; (*F*) keratinocyte chemoattractant (Kc); (*G*) IL-6 (WT Cont n = 6, *Bmpr2*$^{+/-}$ Cont n = 3, WT infected n = 7, *Bmpr2*$^{+/-}$ infected n = 4). Data are presented as mean ± SEM. *$P < 0.05$ compared with WT control, $^{\#}P < 0.05$ compared with *Bmpr2*$^{+/-}$ control, $^{+}P < 0.05$ compared with *Bmpr2*$^{+/-}$ infected. Bmpr2 = bone morphogenetic protein type 2 receptor; Cont = control.

IL-13, Kc, and IL-6 ($P < 0.001$) between WT control and WT infected mice, and a significant increase in serum IL-13 and Kc ($P < 0.001$) between control *Bmpr2*$^{+/-}$ and infected *Bmpr2*$^{+/-}$ mice. We also observed a significant difference in serum IL-6 ($P < 0.01$) between control WT and control *Bmpr2*$^{+/-}$ mice.

In addition, in an *in vitro* assay in which PASMC from WT and *Bmpr2*$^{+/-}$ control mice were cultured with *S. mansoni* eggs for 24 hours, we observed an increase in IL-6 production by the *Bmpr2*$^{+/-}$ PASMC compared with WT PASMC (*see* Figure E4).

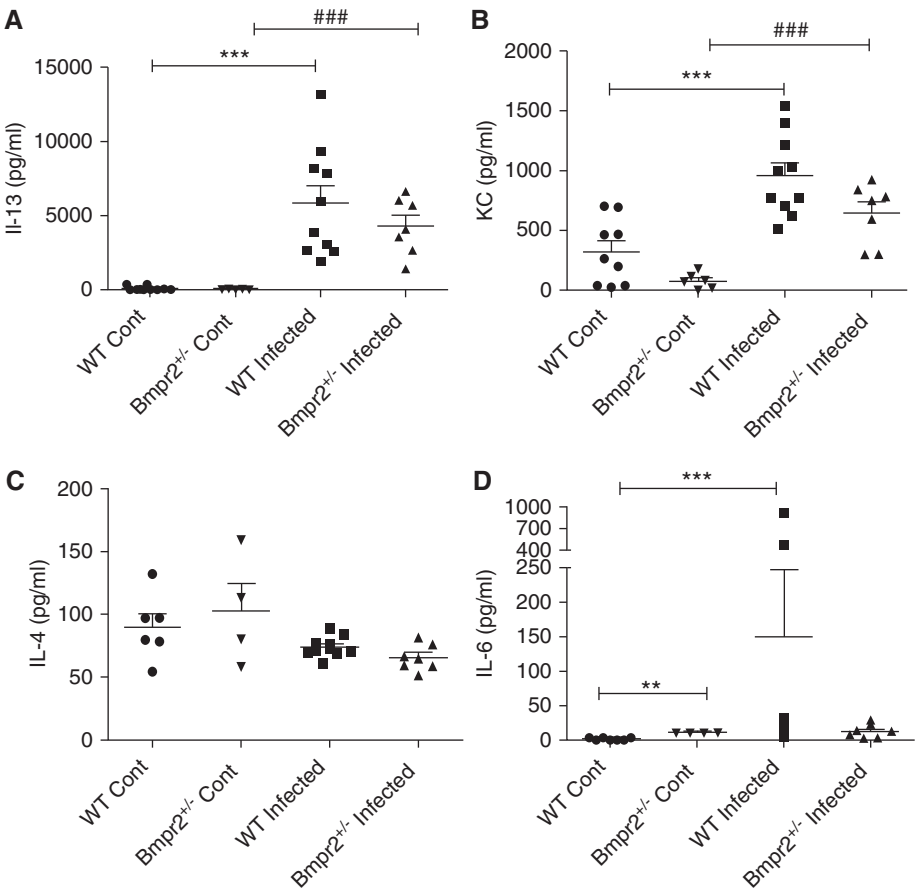

Figure 8. Plots showing serum cytokine profiles in wild-type (WT) and *Bmpr2*$^{+/-}$ control and infected mice. (*A*) IL-13 (WT Cont n = 10, *Bmpr2*$^{+/-}$ Cont n = 5, WT infected n = 10, *Bmpr2*$^{+/-}$ infected n = 7); (*B*) keratinocyte chemoattractant (KC) (WT Cont n = 9, *Bmpr2*$^{+/-}$ Cont n = 6, WT infected n = 10, *Bmpr2*$^{+/-}$ infected n = 7); (*C*) IL-4 (WT Cont n = 6, *Bmpr2*$^{+/-}$ Cont n = 4, WT infected n = 10, *Bmpr2*$^{+/-}$ infected n = 7); (*D*) IL-6 (WT Cont n = 7, *Bmpr2*$^{+/-}$ Cont n = 4, WT infected n = 10, *Bmpr2*$^{+/-}$ infected n = 7). Data are presented as mean ± SEM. $^{**}P < 0.01$ compared with WT control, $^{***}P < 0.001$ compared with WT control, $^{\#\#\#}P < 0.001$ compared with *Bmpr2*$^{+/-}$ control. Bmpr2 = bone morphogenetic protein type 2 receptor; Cont = control.

Increased TGF-β1 Signaling in the Lungs of Infected Mice

There is evidence to suggest that TGF-β1 signaling plays an important role in schistosomiasis-induced PAH (7); we therefore investigated the expression of the downstream markers of TGF-β1 activation, plasminogen activation inhibitor 1 (PAI1) and connective tissue growth factor (CTGF), in the lungs and livers of control and infected mice (Figure 9). We saw no difference in TGF-β1 activation and signaling in the lung tissue between the two genotypes, but we did see a significant increase in both PAI1 ($P < 0.05$) and CTGF ($P < 0.05$) in infected mice compared with their control animals. Similarly, we saw an increase in PAI1 expression in the livers of infected WT mice compared with WT control animals ($P < 0.01$) and in the livers of infected *Bmpr2*$^{+/-}$ mice compared with *Bmpr2*$^{+/-}$ control animals ($P < 0.01$). We saw a trend of an increase in liver CTGF expression in the infected mice compared with the control mice.

Discussion

This study has demonstrated that levels of BMPR-II expression modify the pulmonary vascular response to chronic schistosomiasis. The likely mechanisms involve the increased passage of eggs to the lungs caused by altered remodeling of the hepatic vasculature in *Bmpr2*$^{+/-}$ mice. Indeed, we saw an alteration in the pulmonary and hepatic vasculature, even in control conditions.

The explanation for an increase in pulmonary vascular remodeling in *Bmpr2*$^{+/-}$ mice compared with WT mice is that *Bmpr2*$^{+/-}$ mice had a significantly greater number of eggs in their lungs compared with WT mice. The eggs produced by the female schistosome are highly antigenic and are thought to be responsible for the major pathology associated with the disease (4). The chronic model is mainly a Th2-driven response and the eggs are surrounded by granulomas consisting largely of macrophages and lymphocytes (20, 29). In keeping with the increase in eggs seen in the lungs of the *Bmpr2*$^{+/-}$ mice we also see a significant increase in local inflammatory cytokines. Indeed, we have shown a highly positive correlation between the number of eggs in the lung and lung IL-13 expression and a positive correlation between lung egg count and pulmonary vascular remodeling. We also saw a trend for an increase in lung IL-6 expression in infected *Bmpr2*$^{+/-}$ mice compared with WT infected mice and an increase in IL-6 production in supernatants from PASMC from *Bmpr2*$^{+/-}$ mice that had been cultured with *S. mansoni* eggs for 24 hours *in vitro*. In a previous publication we have shown that PASMC from patients with a mutation in BMPR-2 proliferate in response to IL-6, whereas PASMC from controls did not (30). Importantly, we have also previously shown an increase in the migratory response to TH2 cytokines, particularly IL-13 (6).

Interestingly, we do not see this difference in the liver or in the circulating cytokines. This further supports the hypothesis that it is the local inflammatory response in the lungs that is driving pulmonary vascular remodeling rather than the circulating cytokine levels. In addition, we have shown a significant increase in TGF-β1 signaling in the lungs and livers of infected WT and *Bmpr2*$^{+/-}$ mice. This is particularly interesting because TGF-β1 signaling has been shown to be important in modulating the IL-4 and IL-13 response (7).

The explanation for *Bmpr2*$^{+/-}$ mice having a greater deposition of eggs in the lung compared with WT mice could be either that they have an abnormality in the hepatic vasculature, which enables eggs to more easily access the lung, or a defect in egg clearance of dead eggs. It is reported that 10–20% patients with the

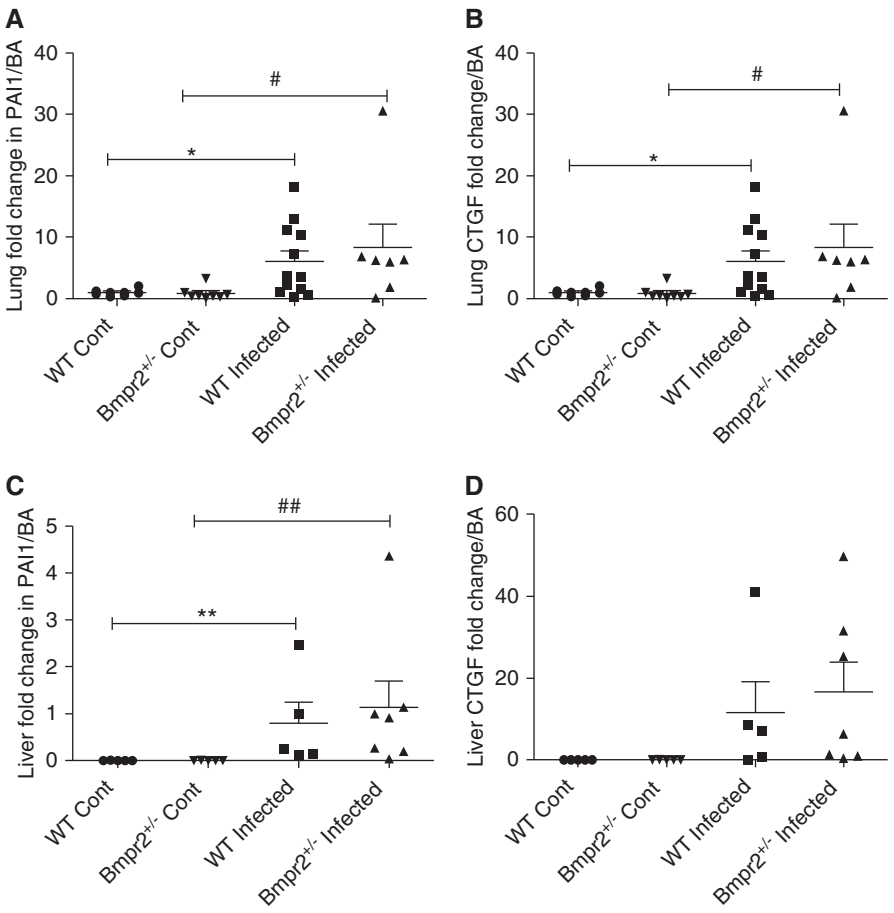

Figure 9. Plots showing expression of downstream transforming growth factor-β1 signaling in the lungs and livers of control and infected wild-type (WT) and *Bmpr2*$^{+/-}$ mice. (*A*) Lung plasminogen activation inhibitor 1 (PAI1) and (*B*) lung connective tissue growth factor (CTGF) (WT Cont n = 8, *Bmpr2*$^{+/-}$ Cont n = 8, WT infected n = 12, *Bmpr2*$^{+/-}$ infected n = 7), (*C*) liver PAI1 (WT Cont n = 5, *Bmpr2*$^{+/-}$ Cont n = 5, WT infected n = 5, *Bmpr2*$^{+/-}$ infected n = 7), and (*D*) liver CTGF (WT Cont n = 5, *Bmpr2*$^{+/-}$ Cont n = 5, WT infected n = 5, *Bmpr2*$^{+/-}$ infected n = 4). Data are presented as mean ± SEM. *$P < 0.05$ compared with WT control, **$P < 0.01$ compared with WT control, $^{\#}P < 0.05$ compared with *Bmpr2*$^{+/-}$ control, $^{\#\#}P < 0.01$ compared with *Bmpr2*$^{+/-}$ control. Bmpr2 = bone morphogenetic protein type 2 receptor; Cont = control.

hepatosplenic form of schistosomiasis mansoni develop PAH (31–33). This is thought to be caused by the opening of portocaval collaterals, in response to an increase in portal pressure, which enables the eggs to be shunted into the lungs (2, 6, 34). Warren and coworkers (34) performed a partial portal vein ligation in a mouse model of *S. mansoni*. They reported that there was a larger number of eggs in the lungs of mice with the partial portal ligation, than in sham operated mice. In addition, portopulmonary hypertension is well documented (35–37). Although we did not measure portal venous pressure, elevated portal venous pressure has been reported previously in mice infected with *S. mansoni* (38–40) and is used as a diagnostic measure in patients with the hepatosplenic form of the disease (41).

Interestingly, mutations in other members of the TGF-β superfamily that are involved in BMPR signaling, such as ALK-1 (the type I receptor that signals in complex with BMPR-II), lead to arteriovenous malformations in several tissues, including the liver, where hepatic arteriovenous malformations can be found (26, 42, 43). The increase in dilatation of the central hepatic vein and hepatic sinusoids in *Bmpr2*$^{+/-}$ mice provides a possible explanation for the increased passage of eggs from the liver to the lungs in these mice. Furthermore, it has been reported that hepatic sinusoids can dilate from 8 to 180 μm in response to locally increased presinusoidal pressure (44).

Egg delivery to the lungs has previously been reported in animals infected with schistosomiasis (34, 45). It has been suggested that portocaval collaterals open as a consequence of an increase in portal pressure, enabling eggs to access the systemic circulation and therefore the lung. However, the presence of collateral vessels has not been actually demonstrated in animal models or in humans infected with schistosomiasis. Blood reaches the liver via two routes: either the hepatic portal vein, carrying blood from the splanchnic circulation, or from the hepatic artery. The hepatic artery runs alongside the portal vein and biliary duct at the periphery of the liver lobule. Arterial blood then flows through the hepatic sinusoids, lined with fenestrated endothelium, and drains into the central hepatic vein, hepatic vein, and finally the inferior vena cava. Warren and coworkers (34) showed that after partial portal vein ligation in a mouse model of schistosomiasis, portal pressure increased along with an increase in egg deposition in the lungs concomitant with a decrease in the number of eggs in the liver. In *Bmpr2*$^{+/-}$ mice we observed an increase in lung egg deposition associated with a significant dilatation of the central hepatic vein along with dilated sinusoids.

One explanation is that the eggs may be able to access the lungs through the opening of extrahepatic portal shunts (46, 47). In the fetus a proportion of blood bypasses the liver and is diverted from the umbilical vein via the ductus venous to the vena cava (47, 48). However, we observed an increase in dilatation of the central hepatic vein with a significant degree of inflammatory infiltrates surrounding the vessel. This suggests that the eggs may be getting through to the inferior vena cava via the hepatic central vein. Indeed, even in noninfected mice we observed a small but significant increase in dilatation of the central hepatic vein in *Bmpr2*$^{+/-}$ mice. However, this does not rule out the possibility that extrahepatic collaterals can also develop.

An alternative explanation for the increase in eggs in the lungs of *Bmpr2*$^{+/-}$ mice might be that there is a defect in egg clearance by the macrophages in these mice. To explore this we performed a macrophage phagocytosis assay. However, the results suggest at baseline that there is

no difference in the ability of macrophages to phagocytose between the *Bmpr2*$^{+/-}$ and WT mice (49).

We have previously shown that a low-dose *S. mansoni* chronic infection for 17 weeks in WT mice leads to a profound degree of pulmonary vascular remodeling that correlates positively with egg burden (5). We have also shown that there is a negative correlation between medial wall thickness and distance of the vessel from an egg (5, 6). In addition, we have shown that in WT mice at 17 weeks postinfection that the degree of pulmonary vascular remodeling is not enough to lead to PAH (5). This has also been shown by others (8). The explanation for this is that egg shunting into the lungs is highly variable and very heterogeneous. However, if the infection is taken out to 25 weeks, where we see a greater egg burden in the lungs, we do see PAH and right ventricular hypertrophy (5). For this particular study 17 weeks was chosen because we questioned whether *Bmpr2*$^{+/-}$ mice might be more susceptible to schistosomiasis-induced pulmonary vascular remodeling. If *Bmpr2*$^{+/-}$ mice were more susceptible this would be more evident at an earlier (17 wk) time point rather than at later time points (e.g., 25 wk), at which point WT mice develop severe pulmonary vascular remodeling and PAH (5).

A limitation of this study is that there is no human evidence to suggest that BMPR2 expression levels are related to PAH severity or presence in human forms of schistosomiasis. However, it is known that there are marked differences in the susceptibility to PAH in patients infected with schistosomiasis. The present study provides an interesting and plausible candidate for human genetic susceptibility studies in PAH associated with schistosomiasis. For example, genetic variation at the *BMPR2* locus leading to reduced BMPR2 expression or function might both increase susceptibility to pulmonary vascular remodeling and promote transhepatic passage of eggs to the lung in these patients. This is worthy of future study in at-risk populations.

In conclusion, we have shown that *Bmpr2*$^{+/-}$ mice have an increased ability for schistosomal eggs to gain access into the lungs. As a consequence there is an increased cytokine expression in the lungs and a greater degree of pulmonary vascular remodeling than seen in the WT mice. The increase of eggs in the lungs of the mutant mice does not seem to be caused by a defect in the macrophage clearance of eggs from the lungs, but seems to be caused by an increased dilatation of the central vein and hepatic sinusoids. This work has shown that genetically determined differences in the remodeling of hepatic veins may represent a new risk factor for PAH associated with schistosomiasis. ■

Author disclosures are available with the text of this article at www.atsjournals.org.

References

1. Alpert JS, Irwin RS, Dalen JE. Pulmonary hypertension. *Curr Probl Cardiol* 1981;5:1–39.
2. Andrade ZA, Andrade SG. Pathogenesis of schistosomal pulmonary arteritis. *Am J Trop Med Hyg* 1970;19:305–310.
3. Bedford DE, Aidaros SM, Girgis B. Bilharzial heart disease in Egypt. *Br Heart J* 1946;8:87.
4. Chirakalwasan N, Coyle CM, Meisner MSJ, Chandra A. Treating a case of severe pulmonary hypertension due to schistosomiasis. *Chest* 2006;130:293S–294S.
5. Crosby A, Jones FM, Kolosionek E, Southwood M, Purvis I, Soon E, Butrous G, Dunne DE, Morrell NW. Praziquantel reverses pulmonary hypertension and vascular remodeling in murine schistosomiasis. *Am J Respir Crit Care Med* 2011;184:467–473.
6. Crosby A, Jones FM, Southwood M, Stewart S, Schermuly R, Butrous G, Dunne DW, Morrell NW. Pulmonary vascular remodeling correlates with lung eggs and cytokines in murine schistosomiasis. *Am J Respir Crit Care Med* 2010;181:279–288.
7. Graham BB, Chabon J, Gebreab L, Poole J, Debella E, Davis L, Tanaka T, Sanders L, Dropcho N, Bandeira A, *et al*. Transforming growth factor-β signaling promotes pulmonary hypertension caused by *Schistosoma mansoni*. *Circulation* 2013;128:1354–1364.
8. Graham BB, Mentink-Kane MM, El-Haddad H, Purnell S, Zhang L, Zaiman A, Redente EF, Riches DW, Hassoun PM, Bandeira A, *et al*. Schistosomiasis-induced experimental pulmonary hypertension: role of interleukin-13 signaling. *Am J Pathol* 2010;177:1549–1561.
9. Morrell NW, Yang X, Upton PD, Jourdan KB, Morgan N, Sheares KK, Trembath RC. Altered growth responses of pulmonary artery smooth muscle cells from patients with primary pulmonary hypertension to transforming growth factor-beta(1) and bone morphogenetic proteins. *Circulation* 2001;104:790–795.
10. Rubin LJ. Primary pulmonary hypertension. *N Engl J Med* 1997;336: 111–117.
11. Sahara M, Sata M, Morita T, Nakamura K, Hirata Y, Nagai R. Diverse contribution of bone marrow-derived cells to vascular remodeling associated with pulmonary arterial hypertension and arterial neointimal formation. *Circulation* 2007;115:509–517.
12. Deng Z, Morse JH, Slager SL, Cuervo N, Moore KJ, Venetos G, Kalachikov S, Cayanis E, Fischer SG, Barst RJ, *et al*. Familial primary pulmonary hypertension (gene PPH1) is caused by mutations in the bone morphogenetic protein receptor-II gene. *Am J Hum Genet* 2000;67:737–744.
13. Lane KB, Machado RD, Pauciulo MW, Thomson JR, Phillips JA III, Loyd JE, Nichols WC, Trembath RC; International PPH Consortium. Heterozygous germline mutations in BMPR2, encoding a TGF-beta receptor, cause familial primary pulmonary hypertension. *Nat Genet* 2000;26:81–84.
14. Machado RD, Pauciulo MW, Thomson JR, Lane KB, Morgan NV, Wheeler L, Phillips JA III, Newman J, Williams D, Galiè N, *et al*. BMPR2 haploinsufficiency as the inherited molecular mechanism for primary pulmonary hypertension. *Am J Hum Genet* 2001;68:92–102.
15. Thomson JR, Machado RD, Pauciulo MW, Morgan NV, Humbert M, Elliott GC, Ward K, Yacoub M, Mikhail G, Rogers P, *et al*. Sporadic primary pulmonary hypertension is associated with germline mutations of the gene encoding BMPR-II, a receptor member of the TGF-beta family. *J Med Genet* 2000;37:741–745.
16. Atkinson C, Stewart S, Upton PD, Machado R, Thomson JR, Trembath RC, Morrell NW. Primary pulmonary hypertension is associated with reduced pulmonary vascular expression of type II bone morphogenetic protein receptor. *Circulation* 2002;105:1672–1678.
17. Long L, Crosby A, Yang X, Southwood M, Upton PD, Kim DK, Morrell NW. Altered bone morphogenetic protein and transforming growth factor-beta signaling in rat models of pulmonary hypertension: potential for activin receptor-like kinase-5 inhibition in prevention and progression of disease. *Circulation* 2009;119:566–576.
18. Morty RE, Nejman B, Kwapiszewska G, Hecker M, Zakrzewicz A, Kouri FM, Peters DM, Dumitrascu R, Seeger W, Knaus P, *et al*. Dysregulated bone morphogenetic protein signaling in monocrotaline-induced pulmonary arterial hypertension. *Arterioscler Thromb Vasc Biol* 2007;27:1072–1078.
19. De Caestecker M, Meyrick B. Bone morphogenetic proteins, genetics and the pathophysiology of primary pulmonary hypertension. *Respir Res* 2001;2:193–197.
20. Mentink-Kane MM, Cheever AW, Thompson RW, Hari DM, Kabatereine NB, Vennervald BJ, Ouma JH, Mwatha JK, Jones FM, Donaldson DD, *et al*. IL-13 receptor alpha 2 down-modulates granulomatous

inflammation and prolongs host survival in schistosomiasis. *Proc Natl Acad Sci USA* 2004;101:586–590.
21. Long L, MacLean MR, Jeffery TK, Morecroft I, Yang X, Rudarakanchana N, Southwood M, James V, Trembath RC, Morrell NW. Serotonin increases susceptibility to pulmonary hypertension in BMPR2-deficient mice. *Circ Res* 2006;98:818–827.
22. Cheever AW. Conditions affecting the accuracy of potassium hydroxide digestion techniques for counting *Schistosoma mansoni* eggs in tissues. *Bull World Health Organ* 1968;39:328–331.
23. Yang X, Long L, Southwood M, Rudarakanchana N, Upton PD, Jeffery TK, Atkinson C, Chen H, Trembath RC, Morrell NW. Dysfunctional Smad signaling contributes to abnormal smooth muscle cell proliferation in familial pulmonary arterial hypertension. *Circ Res* 2005;96:1053–1063.
24. Lopez-De Leon A, Rojkind M. A simple micromethod for collagen and total protein determination in formalin-fixed paraffin-embedded sections. *J Histochem Cytochem* 1985;33:737–743.
25. Hong KH, Lee YJ, Lee E, Park SO, Han C, Beppu H, Li E, Raizada MK, Bloch KD, Oh SP. Genetic ablation of the BMPR2 gene in pulmonary endothelium is sufficient to predispose to pulmonary arterial hypertension. *Circulation* 2008;118:722–730.
26. Liu D, Wang J, Kinzel B, Müeller M, Mao X, Valdez R, Liu Y, Li E. Dosage-dependent requirement of BMP type II receptor for maintenance of vascular integrity. *Blood* 2007;110: 1502–1510.
27. Soon E, Southwood M, Sheares K, Pepke-Zaba J, Morrell NW. Better off blue: BMPR-2 mutation, arteriovenous malformation, and pulmonary arterial hypertension. *Am J Respir Crit Care Med* 2014;189:1435–1436.
28. Wynn TA, Eltoum I, Oswald IP, Cheever AW, Sher A. Endogenous interleukin 12 (IL-12) regulates granuloma formation induced by eggs of *Schistosoma mansoni* and exogenous IL-12 both inhibits and prophylactically immunizes against egg pathology. *J Exp Med* 1994;179:1551–1561.
29. Cheever AW, Lenzi JA, Lenzi HL, Andrade ZA. Experimental models of *Schistosoma mansoni* infection. *Mem Inst Oswaldo Cruz* 2002;97: 917–940.
30. Soon E, Crosby A, Southwood M, Yang P, Tajsic T, Toshner M, Appleby S, Shanahan CM, Bloch KD, Pepke-Zaba J, *et al*. BMPR-II deficiency promotes pulmonary hypertension via increased inflammatory cytokine production. *Am J Respir Crit Care Med* 2015; 192:859–872.
31. Barbosa MM, Lamounier JA, Oliveira EC, Souza MV, Marques DS, Silva AA, Lambertucci JR. Pulmonary hypertension in schistosomiasis mansoni. *Trans R Soc Trop Med Hyg* 1996;90:663–665.
32. Lapa M, Dias B, Jardim C, Fernandes CJ, Dourado PM, Figueiredo M, Farias A, Tsutsui J, Terra-Filho M, Humbert M, *et al*. Cardiopulmonary manifestations of hepatosplenic schistosomiasis. *Circulation* 2009;119:1518–1523.
33. Shaw AFB, Ghareeb AA. The pathogenesis of pulmonary schistosomais in Egypt with special reference to Ayerza's disease. *J Pathol* 1938;46:401–424.
34. Warren KS. Experimental schistosomiasis. *Trans R Soc Trop Med Hyg* 1964;58:228–233.
35. Roberts KE, Fallon MB, Krowka MJ, Brown RS, Trotter JF, Peter I, Tighiouart H, Knowles JA, Rabinowitz D, Benza RL, *et al*.; Pulmonary Vascular Complications of Liver Disease Study Group. Genetic risk factors for portopulmonary hypertension in patients with advanced liver disease. *Am J Respir Crit Care Med* 2009;179:835–842.
36. Medarov BI, Chopra A, Judson MA. Clinical aspects of portopulmonary hypertension. *Respir Med* 2014;108:943–954.
37. Ogawa E, Hori T, Doi H, Segawa H, Uemoto S. Living-donor liver transplantation for moderate or severe porto-pulmonary hypertension accompanied by pulmonary arterial hypertension: a single-centre experience over 2 decades in Japan. *J Hepatobiliary Pancreat Sci* 2012;19:638–649.
38. Costa G, Aguiar BG, Coelho PM, Cunha-Melo JR. On the increase of portal pressure during the acute and chronic phases of murine schistosomiasis mansoni and its reversibility after treatment with oxamniquine. *Acta Trop* 2003;89:13–16.
39. Andrade ZA. Pathogenesis of pipe-stem fibrosis of the liver (experimental observation on murine schistosomiasis). *Mem Inst Oswaldo Cruz* 1987;82:325–334.
40. Vezozzo DC, Farias AQ, Cerri GG, Da Silva LC, Carrilho FJ. Assessment of portal hemodynamics by Doppler ultrasound and of liver morphology in the hepatosplenic and hepatointestinal forms of schistosomiasis mansoni. *Dig Dis Sci* 2006;51:1413–1419.
41. de Toledo CF, Carvente CT, Shigueoka DC, Borges DR. Endothelial markers in schistosomiasis patients with or without portal hypertension. *Dig Dis Sci* 2009;54:1331–1336.
42. Letteboer TG, Mager JJ, Snijder RJ, Koeleman BP, Lindhout D, Ploos van Amstel JK, Westermann CJ. Genotype-phenotype relationship in hereditary haemorrhagic telangiectasia. *J Med Genet* 2006;43: 371–377.
43. Sabbà C, Pasculli G, Lenato GM, Suppressa P, Lastella P, Memeo M, Dicuonzo F, Guant G. Hereditary hemorrhagic telangiectasia: clinical features in ENG and ALK1 mutation carriers. *J Thromb Haemost* 2007;5:1149–1157.
44. Rappaport AM. Hepatic blood flow: morphologic aspects and physiologic regulation. *Int Rev Physiol* 1980;21:1–63.
45. McHugh SM, Coulson PS, Wilson RA. Pathologically induced alterations in the dimensions of the hepatic portal vasculature of mice infected with *Schistosoma mansoni*. *Parasitology* 1987;94:69–80.
46. Wang XX, Zhang FR, Shang YP, Zhu JH, Xie XD, Tao QM, Zhu JH, Chen JZ. Transplantation of autologous endothelial progenitor cells may be beneficial in patients with idiopathic pulmonary arterial hypertension: a pilot randomized controlled trial. *J Am Coll Cardiol* 2007;49:1566–1571.
47. Wilson RA. Leaky livers, portal shunting and immunity to schistosomes. *Parasitol Today* 1990;6:354–358.
48. Cox FE. Schistosomiasis. The mouse that wasn't immune. *Nature* 1990;345:18.
49. Stenger RJ, Warren KS, Johnson EA. An ultrastructural study of hepatic granulomas and schistosome egg shells in murine hepatosplenic schistosomiasis mansoni. *Exp Mol Pathol* 1967;7:116–132.